Abstract# 5335
Posterboard# B0272

Development of OPGx-BEST1 AAV gene therapy for the treatment of bestrophinopathies

Choudhary, Mayur[1], Gray, Alexa[2], Sato, Yu[2], Kwok, Jennifer[2], Arora, Vik[1], Yerxa, Benjamin[1], Cideciyan, Artur[3], Aguirre, Gustavo[2], Beltran, William[2], and Jayagopal, Ashwath[1]

[1]Opus Genetics, Durham, NC, USA

[2]Division of Experimental Retinal Therapies, School of Veterinary Medicine, University of Pennsylvania, Philadelphia, PA 19104, USA

[3]Department of Ophthalmology, Perelman School of Medicine, University of Pennsylvania, , Philadelphia, PA 19104, USA.

Introduction

- BEST1 is a multifunctional, transmembrane channel protein localized to the basolateral membrane of RPE. It has been implicated in anion transport, regulation of calcium signaling and cell volume.[1-4]
- BEST1 gene mutations have been causally associated with a group of retinal disorders, termed bestrophinopathies. Over 200 distinct human BEST1 gene mutations have been reported.[5,6]
- The most common and well-defined juvenile macular dystrophy among the bestrophinopathies is Best vitelliform macular dystrophy (BVMD or Best disease) with an autosomal dominant inheritance (OMIM#153700). Clinically, the disease manifests as bilateral vitelliform lesions, predominantly affecting macular and paramacular areas.[5,7]
- A spectrum of molecular and structural alterations at the RPE-photoreceptor interface triggers formation of vitelliform lesions which lead to photoreceptor degeneration and vision loss.[8,9]
- Proof of concept studies in naturally-occurring dog models of autosomal recessive BEST1 disease (ARB), the closest disease model representative of human bestrophinopathy, caused by mutations in the BEST1 gene have recently shown that a gene augmentation strategy corrects clinically visible subretinal vitelliform lesions as well as diffuse microdetachments.[10,11]
- OPGx-BEST1 is a recombinant AAV2 vector that carries human BEST1 complementary DNA (cDNA) as a single-stranded construct. The plasmid contains a human VMD2 promoter (VMD2), driving the expression of human BEST1.
- **The objective of this study was:**

➢ **To support clinical development of OPGx-BEST1 an AAV-based gene therapy that expresses full length human BEST1 cDNA by determining ocular efficacy and safety in the cmr model of BEST1 disease.**

Materials and Methods

Study Design: The objectives of this study were to conduct a safety and efficacy analysis of OPGx-BEST1 in *BEST1*-mutant dogs. The OPGx-BEST1 vector or vehicle was administered by a single subretinal injection in one eye of *BEST1*-mutant dogs as outlined in **Table 1.** Efficacy endpoints in this study included masked analyses of progression of disease by funduscopic examination, and changes in IS/OS to RPE/tapetum interface distance and changes in ONL thickness (by *in vivo* OCT imaging). Safety endpoints in this study included masked analyses of clinical examination, ophthalmic examination, retinal examination by *in vivo* cSLO/OCT imaging, ERG responses, clinical pathology assessment, immunological and biodistribution analysis, as well as gross pathology and microscopic pathology. A total of 9 animals received the test article or vehicle by subretinal injection in the left eye. The contralateral right eye remained untreated. Animals age ranged from 16-194 weeks at the time of treatment. Both male and female dogs were allocated to each treatment group except for the highest dose group. Animals were allocated to either the vehicle, low dose OPGx-BEST1 or high dose (n=3/group).

Table 1: Study Design

Dose	Number of Animals	Dose Level: Vector Concentration (vg/mL)	Dose Level: Total Dose (vg per eye)	Dose Level: Injection Volume (mL)
High	3	3.0×10^{10}	4.5×10^{9}	~ 0.15
Low	3	9.5×10^{9}	1.4×10^{9}	~ 0.15
Vehicle	3	0	0	~ 0.15

cSLO/OCT imaging: cSLO and OCT imaging was performed with a Spectralis HRA/OCT2 (Heidelberg) unit at pre-dose, 1 week, 4 weeks, 8 weeks, and 12 weeks post-dose. Qualitative assessment of cSLO and single OCT B-scans was performed at all time-points and progression of disease was documented.

ERG: Recordings were conducted at pre-dose and at 11 weeks post-dose utilizing an Espion E3 electroretinography unit (Diagnosys LLC, Lowell, MA). In brief, pupils were dilated with topical atropine sulfate (1%), tropicamide (1%) and phenylephrine (10%). After 20 minutes of dark adaptation, rod- and mixed rod-cone-mediated responses to single 4-ms white flash stimuli of increasing intensities were recorded. Following 5 minutes of white light adaptation, cone-mediated signals to a series of single flashes and to 29.4-Hz flicker stimuli were recorded. The results of the OPGx-BEST1 injected eyes were compared to the vehicle-treated eyes, and to the un-injected contralateral eyes.

Biodistribution: A validated viral shedding/biodistribution assay utilizing qPCR and targeting a distinct sequence of the human BEST1 transgene was developed at CRL, Senneville, QC, Canada.

References

1. Marmorstein AD, Marmorstein LY, Rayborn M, Wang X, Hollyfield JG, Petrukhin K. Bestrophin, the product of the Best vitelliform macular dystrophy gene (VMD2), localizes to the basolateral plasma membrane of the retinal pigment epithelium. *Proc Natl Acad Sci U S A*. 2000; 97: 12758-12763.
2. un H, Tsunenari T, Yau KW, Nathans J. The vitelliform macular dystrophy protein defines a new family of chloride channels. Proc Natl Acad Sci U S A. 2002; 99: 4008-4013.
3. Hartzell HC, Qu Z, Yu K, Xiao Q, Chien LT. Molecular physiology of bestrophins: multifunctional membrane proteins linked to best disease and other retinopathies. Physiol Rev. 2008; 88: 639-672.
4. Strauß O, Müller C, Reichhart N, Tamm ER, Gomez NM. The role of bestrophin-1 in intracellular Ca(2+) signaling. Adv Exp Med Biol. 2014; 801: 113-119.
5. Boon CJ, Klevering BJ, Leroy BP, Hoyng CB, Keunen JE, den Hollander AI. The spectrum of ocular phenotypes caused by mutations in the BEST1 gene. Prog Retin Eye Res. 2009; 28: 187-205.
6. Pasquay C, Wang LF, Lorenz B, Preising MN. Bestrophin 1--Phenotypes and Functional Aspects in Bestrophinopathies. Ophthalmic Genet. 2015; 36: 193-212.
7. Bitner H, Schatz P, Mizrahi-Meissonnier L, Sharon D, Rosenberg T. Frequency, genotype, and clinical spectrum of best vitelliform macular dystrophy: data from a national center in Denmark. Am J Ophthalmol. 2012; 154: 403-412 e404.
8. Bakall B, Radu RA, Stanton JB, Burke JM, McKay BS, Wadelius C, Mullins RF, Stone EM, Travis GH, Marmorstein AD. Enhanced accumulation of A2E in individuals homozygous or heterozygous for mutations in BEST1 (VMD2). Exp Eye Res. 2007; 85: 34-43.
9. Yu K, Qu Z, Cui Y, Hartzell HC. Chloride channel activity of bestrophin mutants associated with mild or late-onset macular degeneration. Invest Ophthalmol Vis Sci. 2007; 48: 4694-4705.
10. Guziewicz KE, Slavik J, Lindauer SJ, Aguirre GD, Zangerl B. Molecular consequences of BEST1 gene mutations in canine multifocal retinopathy predict functional implications for human bestrophinopathies. Invest Ophthalmol Vis Sci. 2011; 52: 4497-4505.
11. Guziewicz KE, Cideciyan AV, Beltran WA, Komaromy AM, Dufour VL, Swider M, Iwabe S, Sumaroka A, Kendrick BT, Ruthel G, Chiodo VA, Heon E, Hauswirth WW, Jacobson SG, Aguirre GD. BEST1 gene therapy corrects a diffuse retina-wide micro-detachment modulated by light exposure. Proc Natl Acad Sci U S A. 2018; 115: E2839-E2848.

Results

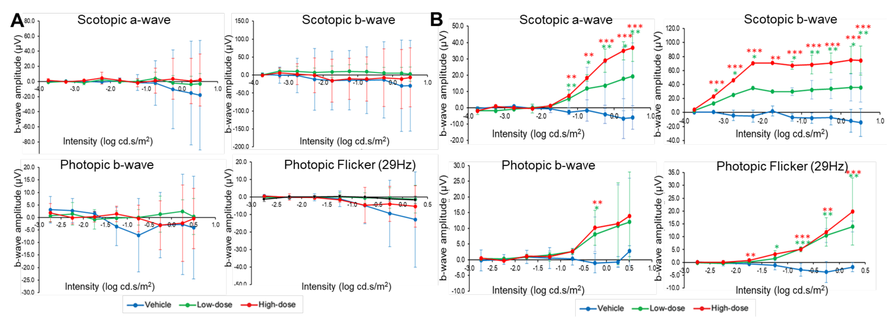

Figure 1. Comparison of ERG amplitudes across treatment groups. Mean (±SD) differences in scotopic a- and b-wave, photopic b-wave and 29-Hz flicker amplitudes between the injected (OS) eyes and un-injected (OD) eyes as a function of intensity of light stimulus, (A) Pre-dose, and (B) 11-weeks post-dose. One-way ANOVA.

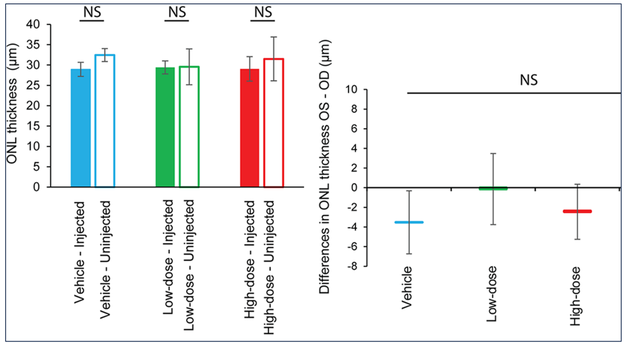

Figure 2. Quantitative analysis of the retention of ONL thickness in the treated area measured by histology at 13 weeks post-dose. (**A**) Mean (± SD) ONL thickness of the treated area of the injected (OS) eyes and of the equivalent area of the un-injected (OD) eyes in the vehicle, low-, and high-dose treatment groups. Paired t-tests; N.S. = non-significant (**B**) Comparison across treatment groups of the mean (± SD) difference in ONL thickness between the treated area of the injected (OS) eyes and the equivalent area of the un-injected (OD) eyes. One-way ANOVA; NS = non-significant.

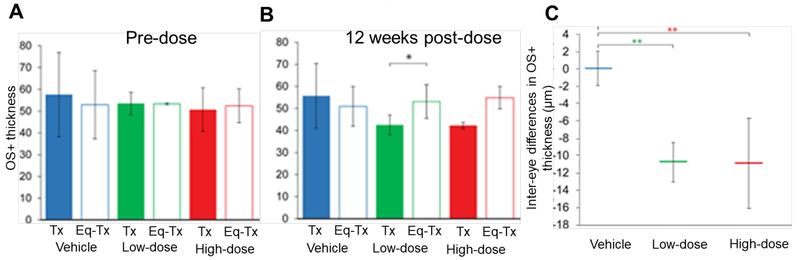

Figure 3. OS+ thickness analysis from Spectralis OCT-derived maps at pre-dose and 12 weeks post-dose. (**A**) Inter-eye comparison within treatment groups of the mean (± SD) OS+ thickness in the treated area of the injected (OS) eyes and the equivalent treated areas of the un-injected/contralateral (OD) eyes (OD) at pre-dose. Analyzed by paired t-test. (**B**) Inter-eye comparison within treatment groups of the mean (± SD) OS+ thickness in the treated area of the injected (OS) eyes and the equivalent treated areas of the un-injected/contralateral (OD) eyes (OD) at 12 weeks post dose. Paired t-test: * = p ≤ 0.05. (**C**) Comparison across treatment groups of the normalized inter-eye difference [IED (OS-OD) at 12weeks - IED (OS-OD) at pre-dose]. Boxed asterisks represent p values from the one-way ANOVA; colored asterisks represent p values of the Bonferroni post-hoc analysis: * = p ≤ 0.05, **= p ≤ 0.01.

Acknowledgments/Disclosures:
This work was partially supported by the Foundation Fighting Blindness (FFB), NIH/NEI RO1 EY006855 and Iveric Bio

Primary Contact:
Mayur Choudhary: MChoudhary@OpusGtx.com
Ben Yerxa: byerxa@OpusGtx.com

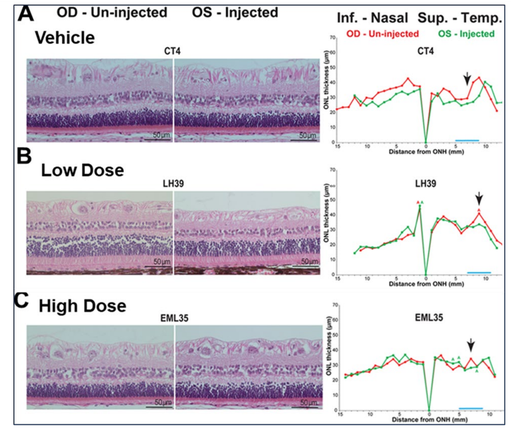

Figure 4. Representative retinal histology and quantification of ONL thickness at 13 weeks post-dose in individual injected and un-injected eyes from all 3 treatment groups. (A) Photomicrographs of H&E stained sections showing the retinal morphology in the treated area of the injected (OS) eye and the equivalent location of the contralateral un-injected (OD) eye. (B) Spidergraphs of ONL thickness measured in both eyes (green traces = OS/injected eye; red traces = OD/un-injected eye) that extend from the optic nerve head (ONH) to the peripheral *ora serrata* along both the inferonasal (Inf. - Nasal) and superotemporal (Sup. – Temp.) quadrants. The section was oriented so as to include the treated area in OS and equivalent area in OD. The blue bar under the x-axis of each spidergraph corresponds to the 5 locations within the treated area (and equivalent area in OD) that were selected for calculation of the mean ONL thickness in the treated area of OS and equivalent area in OD. The black arrows point to the location where the H&E images shown in (A) were taken from. A = artefactual ONL separation during tissue processing.

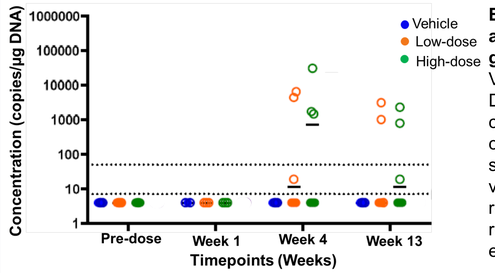

Figure 5. Biodistribution of OPGx-BEST1 in aqueous humor in injected and uninjected eyes from 3 treatment groups. OPGx-BEST1 in the left eye at Vehicle, low-dose and high-dose groups. Dashed line represents the LOD (7.14 copies/µg DNA) and LLOQ (50.00 copies/µg DNA). Negative and positive samples were attributed an arbitrary value of 4 and 19 copies/µg DNA respectively. Closed and open symbols represent data from the right and left eye respectively.

Conclusions

- No electroretinographic abnormalities were seen in any of the OPGx-BEST1 or vehicle-injected eyes. A dose-dependent increase in ERG amplitudes was observed with the low and high-dose cohorts when compared to vehicle.
- Evidence of a significantly lower OS+ thickness (= reduced IS/OS to RPE/T distance) was seen in the treated area of the injected eyes in all (low-dose, and high-dose) treatment groups at 12 weeks post-dose when compared by standard resolution and high-resolution OCT imaging to an equivalent area of the contralateral un-injected eyes.
- Clinical pathology results did not reveal any findings that could be associated with OPGx-BEST1 treatment (data not shown).
- *In vivo* retinal examination by indirect ophthalmoscopy, and cSLO/OCT did not reveal any lesions that could be unambiguously related to OPGx-BEST1 in the eyes injected with the low-, or high-dose.

In conclusion, a single subretinal injection of either doses (1.4 x 10^9, 4.5 x 10^9 vg/eye) of OPGx-BEST1 led to structural and functional improvement in the retinas of BEST1-mutant dogs and did not cause any adverse findings up to 13 weeks after injection.